Valence bonds in elongated boron clusters

Arvanitidis, Athanasios G.; Lim, Kie Zen; Havenith, Remco W. A.; Ceulemans, Arnout

Published in:
International Journal of Quantum Chemistry

DOI:
10.1002/qua.25575

Publication date:
2018

Valence bonds in elongated boron clusters

Athanasios G. Arvanitidis [*], Kie Zen Lim [†],
Remco W.A. Havenith [‡], Arnout Ceulemans [§]

Abstract

A well defined class of planar or quasi-planar elongated boron clusters, of type B_{7+3n}^{q-}, serves as a basis to identify the valence bond picture of delocalized boron networks. The origin of the series is the B_7^- cluster, which exhibits σ-aromaticity. The cluster generating step is the repetitive expansion by three boron atoms in the direction of elongation. Specific electron counting rules are obtained for π-bonding, peripheral σ-bonding and multi-center inner σ-bonding. A valence bond structure is introduced which explains the remarkable regularity in the bonding pattern. The analysis supports 4c-2e bonds as an alternative to the common 3c-2e bonds. The results are validated by symmetry induction and *ab initio* calculations.

[*]Quantum and Physical Chemistry, Department of Chemistry, KULeuven, Celestijnenlaan $200f$, 3001 Leuven, Belgium, athanasios.arvanitidis@kuleuven.be

[†]Theoretical Chemistry, Zernike Institute for Advanced Materials and Stratingh Institute for Chemistry, University of Groningen, 9747 AG Groningen, The Netherlands, Quantum and Physical Chemistry, Department of Chemistry, KULeuven, Celestijnenlaan $200F$, B-3001 Leuven, Belgium

[‡]Theoretical Chemistry, Zernike Institute for Advanced Materials and Stratingh Institute for Chemistry, University of Groningen, 9747 AG Groningen, The Netherlands, Ghent Quantum Chemistry Group Department of Inorganic and Physical Chemistry Ghent University, Krijgslaan 281 (S3) B-9000 Gent, Belgium

[§]Quantum and Physical Chemistry, Department of Chemistry, KULeuven, Celestijnenlaan $200F$, B-3001 Leuven, Belgium, arnout.ceulemans@kuleuven.be

Introduction

The recent literature reports on a wide variety of planar and bowl shaped boron clusters. Proposed structures are usually based on theoretical calculations, but for some cases structures could be confirmed by Photoelectron or infrared spectroscopy [1] on clusters produced by laser evaporation [2–4]. A further special feature of some clusters which are shaped like two concentric rings is the almost barrierless rotatory motion of the inner ring with respect to the outer ring [5]. This motion has been compared to a Wankel motor at the molecular scale [6]. In view of the rich variety of shapes and properties, which challenges accepted concepts of chemical bonding, boron is said to be the new carbon. As opposed to carbon, it is known to adopt multi-center bonds which have to be accomodated in a proper theoretical scheme. [7–9]. To build a consistent valence bond picture that would apply to all these clusters, a gradual approach is required based on a well-defined set of structures. For this, we chose the particular family of the so-called elongated boron clusters. The aim is to obtain a set of rules that rationalize the electronic structure calculations on a series of structures extending from B_7^- to B_{28}^{2-} [10–18].

Elongated Boron Clusters

The origin of the elongated family is B_7^-. Extension of this structure is based on adding B_3 units along a given direction. This leads to a family of B_{7+3n} structures. For n even, stable clusters acquire a closed shell ground-state as mono-anions. For n odd, previous calculations on B_{16} have revealed that it becomes a perfectly planar closed shell structures as a dianion[19]. Here we will report a similar finding for B_{10}^{2-}. On this basis we define the family of elongated boron clusters as the planar or quasi-planar structures with general formula B_{7+3n}^{q-}, with:

$$q = \frac{3-(-1)^n}{2} \tag{1}$$

A set of clusters belonging to this family is shown in Fig.1. Previous calculations on B_{10} show that for the mono-anion the elongated structure ($C_s\,{}^2A''$) is the global minimum[13]. The elongated structure of B_{13}^- was predicted by Boustani to be the global minimum as well[20]. This was later confirmed by Fowler and Ugalde[18]. For the dianion B_{16}^{2-} the elongated

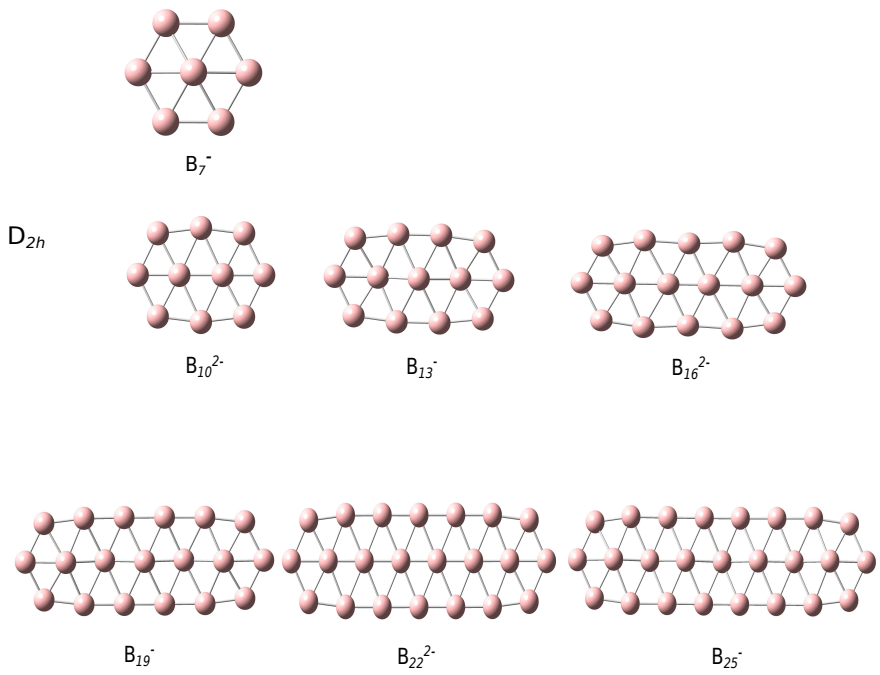

Figure 1: Elongated family up to B_{25}^-

structure ($D_{2h}\,{}^1A_{1g}$) is the minimum at B3LYP and CCSD(T) level of theory[19]. The B_{19}^- cluster is a local minimum ($C_{2v}\,{}^1A_1$)[21]. At LDA level it is 7 kcal/mol above a disk-like structure which is the global minimum. For B_{22} cluster the mono-anion was investigated by Zope et al. at PBE level[22]. It was found to be the second lowest minimum, 5.5 kcal/mol above a double-ring structure. Sergeeva et al.[11] proposed for the global minimum of this cluster an anthracene-like planar structure, but did not investigate the elongated isomer. Finally the elongated form of B_{25}^- is competing with bowl-shaped alternatives with a marginal difference of only 0.9 kcal/mol at CCSD(T)/6-311+G(d)//PBE0/6-311+G(d) level[12].

Methods

In this paper we will investigate in detail a set of 8 clusters, from B_7^- till B_{28}^{2-}. For each cluster we perform a geometry optimization and detailed electronic structure calculations using Density Functional Theory (DFT) methods. All clusters are optimized at the B3LYP/6-311$G**$ level of theory[23–25] and are confirmed as local minima by calculation of vibrational

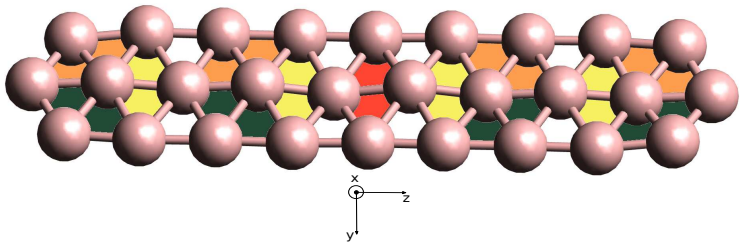

Figure 2: The B_{28}^{2-} cluster, with C_{2h} symmetry. The color segments describe 4c-2e bonds

frequencies using the G09 package[26]. For dianions some test calculations were also performed with the inclusion of diffuse functions, at the B3LYP/6-311 + $+G**$ level. To describe the electron distribution in chemical systems, a variety of indices have been proposed, all of them carrying their pros and cons. In this paper we have opted for the Adaptive Natural Density Partitioning (AdNDP) analysis[27–29], which provides a quantitative and comprehensive picture of bonding in many non-classical chemical structures including boron clusters. In previous papers, AdNDP has been used successfully to examine bonding patterns in a variety of boron clusters. The bonding analysis was carried out using the AdNDP method at the B3LYP/6-311$G**$ level of theory as implemented in Multiwfn software[30]. In addition some test calculations were carried out with other functionals (PBE0, PBE, M06, TPSSh) to examine the stability of the AdNDP occupation numbers. Canonical molecular orbitals were visualized using Avogadro[31] and AdNDP bonds using Molden[32] and Gaussview software. The orbital composition of the resulting ground states is classified according to the irreducible representation of a standard D_{2h} symmetry group. The in-plane directions are labeled as z and y for the long and short axis respectively. The x direction coincides with a twofold rotation axis perpendicular to the plane of the molecule, as indicated in Fig.2. In Figure 1 we show the optimized geometry of the largest cluster of our series, with $n = 7$. The accurate symmetry is C_{2h} due to some ruffling of the inner boron chain.

Results

Electron counting rules

The total number of valence electrons in the clusters under investigation is $3(7+3n)+q$. Our strategy to find out the bonding rules of these electrons is based on reverse engineering. Table 1 shows how this total electron count can be distributed over several types of bonding. First of all, since all clusters are quasi-planar or exactly planar, the valence orbitals can be partitioned in a π and a σ shell. As we have shown before, the π-bonding is of multi-center character and follows the simple particle in an elongated box model[33,34]. B_7^- has only two π bonds, and therefore is anti-aromatic as far as π-aromaticity is concerned. Equal occupation of the π_x and π_y orbitals gives rise to a triplet ground state, which favors an hexagonal pyramidal geometry, with C_{6v} symmetry. In contrast unequal occupation of both orbitals leads to a distorted C_{2v} structure with a singlet ground state[13,35]. Both spin states are nearly degenerate. In the elongated clusters the singlet C_{2v} structure will prevail, but - irrespective of whether one considers the singlet or the triplet state - B_7^- counts for two bonds. For the higher homologues the number of π bonds increases in a perfectly linear relation to the extension of the cluster, and corresponds simply to $n+2$; so each added B_3 unit introduces one additional π bond to the two bonds of the $n=0$ member. The remainder electron count has to be assigned to in-plane σ-bonding. One thus has:

$$\begin{aligned} N_{total} &= 3(7+3n)+q \\ N_{\pi} &= 2n+4 \\ N_{\sigma} &= N_{total}-N_{\pi} = 17+7n+q \end{aligned} \tag{2}$$

Hence the challenge really concentrates on the σ-bonds. Here AdNDP provides an important insight. The search for localized electron-pair bonds between two B atoms (2c-2e bonds) has revealed that the perimeter of the cluster always forms a totally bonding ring. Thus, although boron clusters are electron-deficient, they nevertheless invest in localized bonding on the perimeter. This is not only true for the elongated clusters, studied in this report, but also holds for many other templates[36]. Closer inspection of the molecular orbitals involved indicates that the corresponding electron density is not restricted to pure 2c-2e bonds but

n	B^{q-}_{7+3n}	N_{total}	N_π	N_σ	$N_{\sigma o}$	$N_{\sigma i}$
0	B_7^-	22	4	18	12	6
1	B_{10}^{2-}	32	6	26	16	10
2	B_{13}^-	40	8	32	20	12
3	B_{16}^{2-}	50	10	40	24	16
4	B_{19}^-	58	12	46	28	18
5	B_{22}^{2-}	68	14	54	32	22
6	B_{25}^-	76	16	60	36	24
7	B_{28}^{2-}	86	18	68	40	28

Table 1: Elongated boron clusters: valence electron counts, with a partitioning over π, outer σ and inner σ bonds.

also includes some outward-pointing lone-pair character. We have investigated this further for the case of the B_{10}^{2-} dianion, including diffuse basis functions. This stabilizes the energy by a marginal 0.48 eV, but the molecular orbitals and electron density distribution are not affected at all. The total in-plane bonding in each cluster can thus be considered as a sum of two main "fractions": the totally bonding outer perimeter (including outward lone-pairs) and the remainder responsible for inner bonding. The latter bonding must necessarily be delocalized since the remaining number of electrons is insufficient to link all inner boron atoms by 2c-2e bonds. The electron count for the 2c-2e bonds in the outer fraction is denoted as $N_{\sigma o}$. Note that there are six outer bonds in B_7 and that for each n an additional two outer bonds are added. Hence in total there are $6+2n$ perimeter bonds. So $N_{\sigma o}$ is equal to twice that number. The remainder is the inner bonding count, denoted as $N_{\sigma i}$:

$$\begin{aligned} N_{\sigma o} &= 12 + 4n \\ N_{\sigma i} &= N_\sigma - N_{\sigma o} = 5 + 3n + q \end{aligned} \tag{3}$$

These numbers can be found in Table 1. It is intriguing to find that the delocalized bonding follows a peculiar regularity, the number of electrons going up alternately by four and by two, as: 6, 10, 12, 16, 18, 22, 24, 28. As a consequence of this regularity, the inner σ-count for even values of n is a multiple of six, while for odd values of n it is exactly equal to

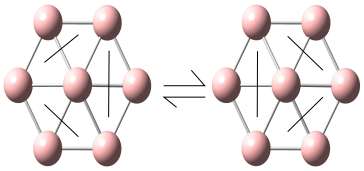

Figure 3: Resonance in B_7^- adopting the 4c-2e partitioning

the number of boron atoms! To understand how the electron deficient boron succeeds in providing such a regular delocalized bonding scheme over the cluster interior forms the main topic of this paper.

Delocalized bonding

Boron is known for its tendency to form triangular 3c-2e bonds, so it is a good starting point for the AdNDP analysis to search for local three-center bonds. For the case of B_{16}^{2-} Sergeeva et al.[19] identified four isolated inner triangles, with occupation numbers above 1.86 $|e|$. The remaining two electron pairs were allocated to 4c-2e bonds on either side, with occupation numbers up to 1.97 $|e|$. This scheme explains the 16 inner electrons, as counted in Table 1. However, when one tries to apply the same pattern to the other members of the cluster, discrepancies arise both for smaller and larger n. Indeed, adding or subtracting a B_3 unit in this scheme accounts for a change by 4 in the inner electron count. Extension of the model by Sergeeva et al. for arbitrary n is expressed by the quantity Q_σ:

$$Q_\sigma = 4 + 4n \tag{4}$$

As shown in Table 2 this quantity does not match the $N_{\sigma i}$ result, except for $n = 2, 3$. So a more general scheme is needed. We note that according to the Q_σ count in Table 2, the starting cluster of the series, B_7^-, is assigned only two bond pairs, while it actually has three electron pairs for inner σ-bonding. This strongly suggests that this bonding could be σ-aromatic and provides a central clue that 4c-2e rather than 3c-2e bonds should be at the basis of the delocalized bonding. The hexagon around the central boron in this cluster contains six rhombic four-center units, such that the partitioning of three 4c-2e pairs over this hexagon will make up two Kekule-type combinations as shown in Fig.3. Their resonance

n	B	$N_{\sigma i}$	Q_σ
0	B_7^-	6	4
1	B_{10}^{2-}	10	8
2	B_{13}^-	12	**12**
3	B_{16}^{2-}	16	**16**
4	B_{19}^-	18	20
5	B_{22}^{2-}	22	24
6	B_{25}^-	24	28
7	B_{28}^{2-}	28	32

Table 2: Inner σ-bonds: comparison of actual electron count ($N_{\sigma i}$) versus the number of electrons in a localized scheme of triangular bonds, with two 4c-2e bonds at the outsides.

leads to a fully delocalized 3σ aromatic sextet. Thus, a viable hypothesis is to base the bonding pattern on *isolated stable hexagonal units* in the boron network. In this hypothesis there is a clear distinction between clusters with even and odd n. For n even, clusters are mono-anionic, hence $q = 1$, and the number of inner σ electrons is equal to $6 + 3n$. This is a multiple of 6, and indeed these clusters can be partitioned in isolated σ-aromatic rings. Note that in this pattern neighboring hexagons share a common vertex, leaving two non-bonding triangles in between. This partitioning scheme is illustrated in Fig.4. For n odd, a perfect partitioning in isolated hexagons falls short of two hexagons sharing a common bond. These clusters can thus be partitioned in isolated hexagons, *and* two additional 4c-2e bonds, as shown in Fig.4. Such unequal distribution of density thus requires to adopt resonance as an essential ingredient of the bonding. The smallest cluster of this type is B_{10}^{2-}. Keeping the 4c-2e partitioning, this cluster matches the topology of naphthalene, and one can identify the five bonding combinations as the five double bonds in the three resonating Kekule forms of this carbon analogue. This fits the expected electron count of 10. Hence the increase of n by one, from $n = 0$ to $n = 1$, gives rise to four extra electrons. Then from $n = 1$ to $n = 2$ only two more electrons are needed to make up for an additional aromatic sextet. Following the same partition, the $N_{\sigma i}$ counts for B_{16}^{2-} and B_{22}^{2-} are 16 and 22, respectively. Indeed one

can easily show that, for n odd, the number of delocalized σ electrons exactly equals the number of boron atoms.

$$\text{for n odd: } N_{\sigma i} = 3(n+1) + 4 = 7 + 3n \tag{5}$$

Molecular orbital symmetries

The proposed bonding schemes comply with the electron counts, but this mere coincidence can hardly be considered as a proof for the validity of these claims. AdNDP analysis in itself is not conclusive either, since all 3c-2e and 4c-2e bonds, as obtained by AdNDP, usually have occupation numbers above a threshold of 1.6 $|e|$. However the proposed bonding scheme uses only a subset of all possible triangular and rhombic bonds, and invokes resonance to cover the whole atomic mesh. Hence for a more direct proof of the proposed scheme, we need to identify the symmetries of the localized bonds that correspond to the proposed pattern, and compare these to the symmetries of the MO's, obtained from the DFT calculation. Quasi-planar clusters with C_{2h} symmetries were reoptimized under a D_{2h} constraint, so as to maximize symmetry information. The reason why we chose to do the analysis in the idealized planar group is based on a simple group-theoretical argument: if the prediction of the irreducible representations of the occupied MOs can be shown to hold in the covering group, it will necessarily be obeyed in the subgroups, while the opposite is not the case. In this symmetry, the plane of the molecule is identified as the σ_{yz} reflection plane, with the z-defined by a C_2^z axis coinciding with the major axis of the molecule. The symmetries of localized bonds are generated by the *induction method*[37]. For in-plane bonds, three types of inductions are possible. The induction process takes an object at a particular site of the molecule, and generates all its symmetry related copies. Here the object is a valence bond, localized on a given site. Such a bond is a totally symmetric object in the site symmetry and is labeled as an a-type irreducible representation in the site group. This is shown schematically in Fig.5. In case of a central bond, the induction is trivial since the site group coincides with D_{2h} and all symmetry elements will map it onto itself. Such a bond thus transforms as the totally symmetric irreducible representation in D_{2h}, and receives the label

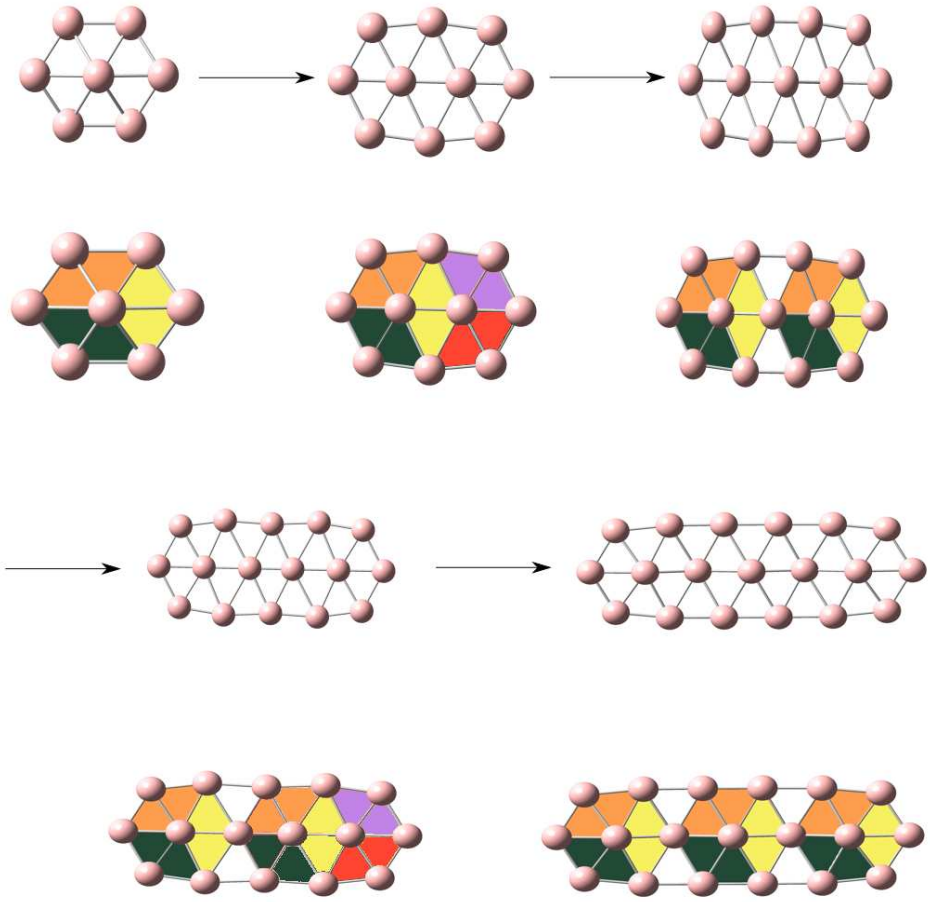

Figure 4: Covering the elongated boron clusters by 4c-2e bonds. The first, third, fifth, ...member consist of isolated aromatic sextets with three 4c-2e bonds, indicated in yellow, orange and green. The second, fourth, ...member always have an additional pair of 4c-2e bonds, indicated in red and blue.

n	B	Peripheral 2c-bonds	A_g	B_{3g}	B_{1u}	B_{2u}
0	B_7^-	$O_3 + O_4$	2	1	1	2
1	B_{10}^{2-}	$2O_4$	2	2	2	2
2	B_{13}^-	$O_3 + 2O_4$	3	2	2	3
3	B_{16}^{2-}	$3O_4$	3	3	3	3
4	B_{19}^-	$O_3 + 3O_4$	4	3	3	4
5	B_{22}^{2-}	$4O_4$	4	4	4	4
6	B_{25}^-	$O_3 + 4O_4$	5	4	4	5
7	B_{28}^{2-}	$5O_4$	5	5	5	5

Table 3: Symmetry orbits for the peripheral outer σ-bonds

A_g. This trivial orbit is denoted as O_1. A bond which is cut by the z-axis, but is off-center, has two copies at either side of the center of inversion. Their symmetries are given by the induction from the C_{2v}^z subgroup, and correspond to orbit O_2. Similarly, a perimeter bond which is lying on the y-axis has a symmetry related mirror image at the opposite side of the perimeter, as obtained by induction from the C_{2v}^y subgroup. This is orbit O_3. Finally, for a bond which is not lying on a twofold symmetry axis and has only in-plane reflection symmetry, there are four identical copies, the symmetries of which are obtained by induction from C_s^{yz}, as in orbit O_4. The induced irreducible representations are indicated by capital letters, and form four *o*rbits:

$$\begin{aligned} O_1 = \Gamma(a_g\, D_{2h} \uparrow D_{2h}) &= A_g \\ O_2 = \Gamma(a_1\, C_{2v}^z \uparrow D_{2h}) &= A_g + B_{1u} \\ O_3 = \Gamma(a_1\, C_{2v}^y \uparrow D_{2h}) &= A_g + B_{2u} \\ O_4 = \Gamma(a'\, C_s^{yz} \uparrow D_{2h}) &= A_g + B_{3g} + B_{1u} + B_{2u} \end{aligned} \tag{6}$$

In Table 3 are listed the symmetry orbits for the peripheral bonds. In order to determine the symmetry for the multi-center *inner* bonds, we have to take into account the difference between clusters with even n which are σ-aromatic, and the ones with odd n. In the aromatic B_7^- cluster the usual three bonding molecular orbitals are found, which are already adapted

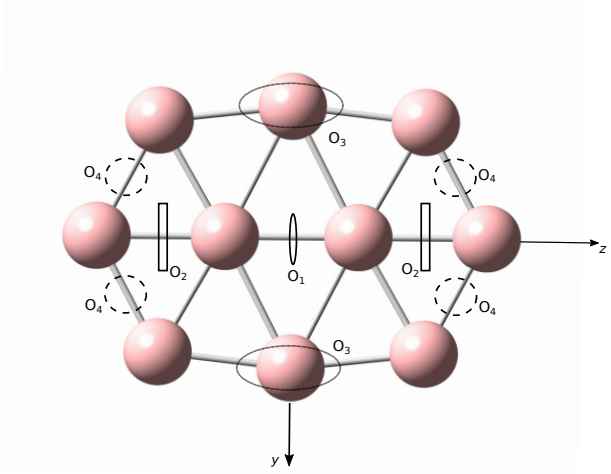

Figure 5: O_1 up to O_4 orbits for B_{10}^{2-}

to the point-group symmetry: the nodeless totally symmetric $6c$ orbital, has A_g symmetry, and the two degenerate orbitals with one nodal plane transform as $B_{1u} + B_{2u}$. We denote these irreducible representations of a central sextet hexagon by capital letter S.

$$S = A_g + B_{1u} + B_{2u} \tag{7}$$

For aromatic rings lying off-center, such as in B_{13}^{-}, induction now involves site objects which are not yet adapted to the full point group symmetry. The $6c$ fully bonding orbital is totally symmetric in the C_{2v}^{z} sitegroup and thus induces the O_2 orbit. This is also the case for the combination which has a nodal plane perpendicular to the z-axis, since this plane does not coincide with a reflection plane of the central point group. However for the remaining combination the nodal plane coincides with the σ_{xz} reflection plane, indicating that this combination has b_2 symmetry in the C_{2v}^{z} site group. This gives rise to a further orbit, as depicted in Fig.6. In this way all orbital symmetries of delocalized σ bonds for clusters with even n are easily obtained, as given in Table 4.

$$O_5 = \Gamma(b_2\, C_{2v}^{z} \uparrow D_{2h}) = B_{3g} + B_{2u} \tag{8}$$

To identify the orbital symmetries of the members with n odd, we must make a distinction between two subclasses: the first subclass is formed by the series B_{10+12m}^{2-} (with $m = 0, 1, ...$), as exemplified by the clusters B_{10}^{2-} and B_{22}^{2-}, while the second subclass is defined as B_{16+12m}^{2-}, with B_{16}^{2-} as its first member. Starting with B_{10}^{2-}, to find the symmetry of its five delocalized

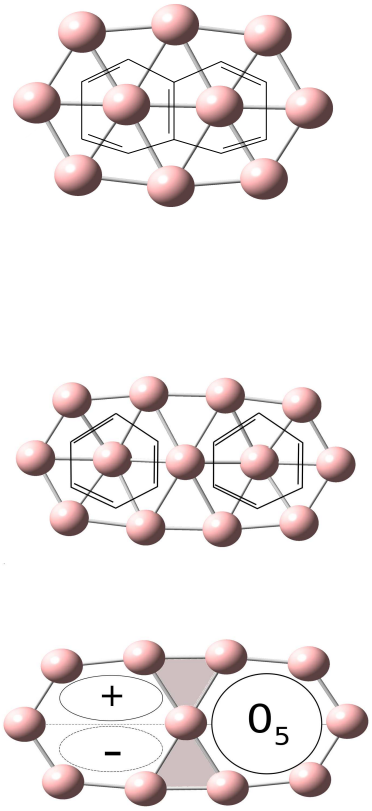

Figure 6: Schematic σ-aromatic structures in B_{10}^{2-} and B_{13}^{-}. The 4c-2e bonds are put in correspondence to double bonds of hydrocarbons. In B_{10}^{2-} (top), a Kekule structure of napthalene is produced. In B_{13}^{-} (middle) the 4c-2e bond corresponds to two isolated benzenes. The b_2 orbital of B_{13}^{-} (bottom) gives rise to the O_5 orbit.

n	B	Inner 4c-bonds	A_g	B_{3g}	B_{1u}	B_{2u}
0	B_7^-	S	1	0	1	1
1	B_{10}^{2-}	$O_1 + O_4$	2	1	1	1
2	B_{13}^-	$2O_2 + O_5$	2	1	2	1
3	B_{16}^{2-}	$O_2 + O_3 + O_4$	3	1	2	2
4	B_{19}^-	$S + 2O_2 + O_5$	3	1	3	2
5	B_{22}^{2-}	$O_1 + O_2 + 2O_4$	4	2	3	1
6	B_{25}^-	$4O_2 + 2O_5$	4	2	4	2
7	B_{28}^{2-}	$3O_2 + O_3 + O_4 + O_5$	5	2	4	3

Table 4: Symmetry orbits for the delocalized inner σ-bonds

inner σ-bonds, we rely on the analogy with conjugated carbon analogues. As shown before its electronic structure corresponds to an aromatic sextet, to which two extra bonds are added. The corresponding carbon analogue is thus identified as naphthalene, which has three resonating Kekule structures. However two of these are broken symmetry solutions. In order to determine the symmetry orbits, we thus must choose the unique Kekule structure that is invariant under the D_{2h} symmetry, as shown in Fig.6. From this structure the 4c-2e bonds can be identified as the $O_1 + O_4$ orbits. The next odd n member of this subclass, B_{22}^{2-}, can then immediately be described as a central B_{10} unit with two aromatic sextet at either side, so we could formally write $B_{22} = B_{10} + 2B_7$, or in general:

$$B_{10+12m} = B_{10+12(m-1)} + 2B_7 \tag{9}$$

The remaining series, B_{16+12m}^{2-}, starts out at B_{16}^{2-}. According to the scheme in Fig.4, this would correspond to the sum of B_{10}^{2-} and one aromatic sextet, yielding indeed 8 delocalized σ-orbitals. However, there is no conjugated hydrocarbon that would combine a phenyl and a naphthyl in a centrosymmetric way. Hence to account for the eight orbitals and keep D_{2h} symmetry, we formally partition B_{16}^{2-} as two aromatic sextets at either side, and two 3c-2e bonds in the center, thus approaching the valence bonds proposed previously by Boldyrev et al[19]. The corresponding symmetry induction is given in Table 3. This building-up principle can then easily be extended to the next member B_{28}^{2-}, which can be summarized

as: $B_{28} = B_{16} + 2B_7$, or in general:

$$B_{16+12m} = B_{16+12(m-1)} + 2B_7 \tag{10}$$

In this way the symmetries of the entire set of σ orbitals can be characterized by four integer numbers, describing the frequencies of the allowed irreducible representations of the D_{2h} symmetry group:

$$\Gamma_\sigma = c_1 A_g + c_2 B_{3g} + c_3 B_{1u} + c_4 B_{2u} \tag{11}$$

These numbers are obtained by adding the results for peripheral and central in-plane bonds in Tables 3 and 4 respectively. As an example, for the largest cluster of our series, one finds:

$$\Gamma_\sigma(B_{28}^{2-}) = 10A_g + 7B_{3g} + 9B_{1u} + 8B_{2u} \tag{12}$$

The corresponding orbitals, calculated by DFT, are all listed with their symmetries in D_{2h} in the supplementary material. There is exact correspondence between Γ_σ and the calculated symmetries. Since in this analysis each cluster is uniquely identified by a code of four integer numbers, this observed total eclipse provides a strong proof for the proposed valence bond structure.

Discussion

The proposed decomposition of the valence bonds in these elongated clusters can be further analyzed using the AdNDP technique. In Fig.7 we provide the AdNDP analysis of B_{13}^-. This is one of the two clusters, which according to Table 2 can equally well be split into eight 4c-2e or 3c-2e bonds. Table 5 lists corresponding density amounts for several resonance structures with 4c-2e and 3c-2e schemes. The residues are the remaining densities, that are not accounted for by the proposed partitioning. The results all refer to calculations with the B3LYP functional. Application of other functionals did not affect the occupation numbers, changes being limited to 0.1 %. It is seen that the 4c-2e bonding leaves less unrecovered amount of the total density. As expected, the AdNDP analysis recovers the ten peripheral 2c-2e bonds. As for the internal four-center bonds, the B_{13}^- network contains 16 four-center

units formed by two triangles sharing a common edge. Of these, exactly 12 have an electron occupation larger than a threshold of 1.87 $|e|$, while the occupation of the four remaining ones cannot be detected up to a threshold 1.87 $|e|$. The twelve dominant 4c-2e bonds precisely constitute all the possible Kekule structures that can be drawn from two isolated hexagons, as indicated by the color scheme in Table 5. We thus claim that AdNDP analysis supports the proposed bonding scheme of two Clar aromatic sextets. In this interpretation AdNDP yields the basic Kekule patterns on which resonance is to be applied[38]. The Table also offers a comparison with the strictly localized scheme, consisting of two 4c-2e bonds at either side, and four internal 3c-2e bonds. It is seen that the 4c-2e bonding leaves less unrecovered amount of the total density. The arrangement of the inner σ electrons in 4c-2e bonds grants higher occupation numbers and confirms the low occupation numbers for the unused triangles in agreement with the ideal D_{2h} symmetry.

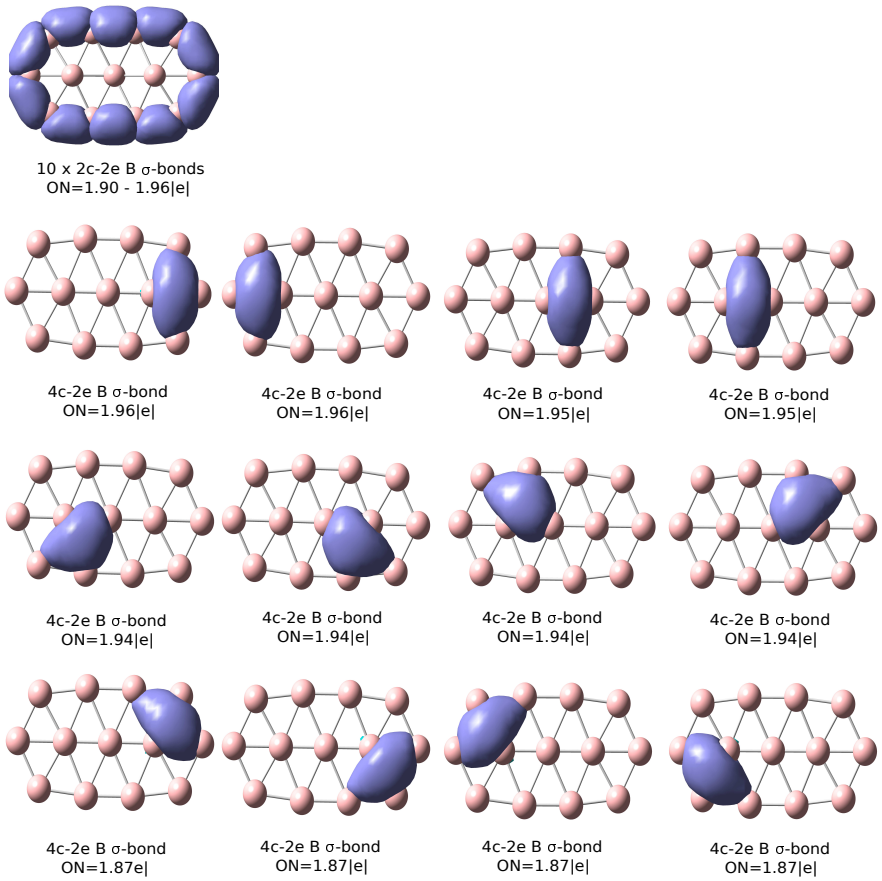

Figure 7: AdNDP analysis of the σ bonds in B_{13}^{-}, showing ten localized peripheral bonds, and twelve four-center bonds with an occupation number exceeding 1.87 $|e|$

The arrangement of the inner σ electrons in 4c-2e bonds grants higher occupation numbers and confirms the low occupation numbers for the unused triangles in agreement with the ideal D_{2h} symmetry.

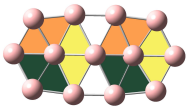
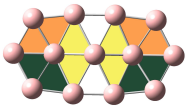
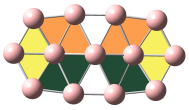
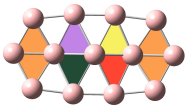

	inner 1	inner 2	inner 3	3c-2e inner
2c-2e σ-bonds	18.81	18.81	18.81	18.81
4c-2e/3c-2e σ-bonds	11.40	11.25	11.51	11.14
π-bonds	7.18	7.18	7.18	7.18
residue	2.65	2.80	2.54	2.91

Table 5: Resonance structures in B_{13}^-

Conclusion

Electron counting rules for small elongated boron clusters are provided to rationalize the preference of boron for multi-center bonding. The rules can be summarized as follows: chemical bonding in the family of B_{7+3n}^{q-} comprises three levels:

1. Delocalized π-bonding: the number of bonding combinations is equal to $n+2$ and closely follows the orbital scheme of a particle in a rectangular box.

2. Localized σ-bonding at the outside: the perimeter of the cluster always consists of a $(6+2n)$-membered chain of localized 2c-2e bonds.

3. Delocalized σ-bonding at the inside: Three subclasses are identified:

   (a) Clusters of type B_{7+6m}^- comprise $m+1$ isolated σ-aromatic sextets.

   (b) Clusters of type B_{10+12m}^{2-}: their inner electron count is equal to the number of boron atoms and consists of a 10-electron naphthalene like structure and $2m$ aromatic sextets.

   (c) Clusters of type B_{16+12m}^{2-}: their inner electron count is equal to the number of boron atoms and consists of $2m$ isolated σ-aromatic sextets and two central 3c-2e bonds.

These findings emphasize the dominance of σ-aromaticity in these clusters. The patterns for the inner delocalized bonding are essentially based on 4c-2e bonds and are supported

by symmetry induction and by ab initio analysis with the AdNDP technique. Those 4c-2e regularities are valid for elongated boron clusters but we expect them to be useful as well for more complex cases with different topologies.

Acknowledgments

AGA thanks the Flemish Science Fund(FWO) for financial support. AGA is indebted to Prof.Alexander Boldyrev and Dr.Ivan Popov for fruitful conversations, the accommodation and the facilities provided during the stay of AGA in Utah State University.

References

1. L.-S. Wang, The Journal of Chemical Physics **143**, 040901 (2015).

2. S. J. L. Placa, P. A. Roland, and J. J. Wynne, Chemical Physics Letters **190**, 163 (1992).

3. L. Hanley and S. L. Anderson, The Journal of Physical Chemistry **91**, 5161 (1987).

4. L. Hanley, J. L. Whitten, and S. L. Anderson, The Journal of Physical Chemistry **92**, 5803 (1988).

5. S. Jalife, L. Liu, S. Pan, J. L. Cabellos, E. Osorio, C. Lu, T. Heine, K. J. Donald, and G. Merino, Nanoscale **8**, 17639 (2016).

6. J. O. C. Jiménez-Halla, R. Islas, T. Heine, and G. Merino, Angewandte Chemie International Edition **49**, 5668 (2010).

7. I. A. Popov and A. I. Boldyrev, *Classical and Multicenter Bonding in Boron: Two Faces of Boron* (Springer International Publishing, Cham, 2015), pp. 1–16.

8. T. B. Tai, A. Ceulemans, and M. T. Nguyen, Chemistry A European Journal **18**, 4510 (2012).

9. E. Oger, N. R. M. Crawford, R. Kelting, P. Weis, M. M. Kappes, and R. Ahlrichs, Angewandte Chemie International Edition **46**, 8503 (2007).

10. W. Huang, A. P. Sergeeva, H.-J. Zhai, B. B. Averkiev, L.-S. Wang, and A. I. Boldyrev, Nat Chem **2**, 202 (2010), ISSN 1755-4330.

11. A. P. Sergeeva, Z. A. Piazza, C. Romanescu, W.-L. Li, A. I. Boldyrev, and L.-S. Wang, Journal of the American Chemical Society **134**, 18065 (2012).

12. Z. A. Piazza, I. A. Popov, W.-L. Li, R. Pal, X. C. Zeng, A. I. Boldyrev, and L.-S. Wang, The Journal of Chemical Physics **141**, 034303 (2014).

13. T. B. Tai, D. J. Grant, M. T. Nguyen, and D. A. Dixon, The Journal of Physical Chemistry A **114**, 994 (2010).

14. T. B. Tai, N. M. Tam, and M. T. Nguyen, Chemical Physics Letters **530**, 71 (2012), ISSN 0009-2614.

15. T. B. Tai, N. M. Tam, and M. T. Nguyen, Theoretical Chemistry Accounts **131**, 1241 (2012).

16. J.-i. Aihara, The Journal of Physical Chemistry A **105**, 5486 (2001).

17. J.-i. Aihara, H. Kanno, and T. Ishida, Journal of the American Chemical Society **127**, 13324 (2005).

18. J. E. Fowler and J. M. Ugalde, The Journal of Physical Chemistry A **104**, 397 (2000).

19. A. P. Sergeeva, D. Y. Zubarev, H.-J. Zhai, A. I. Boldyrev, and L.-S. Wang, Journal of the American Chemical Society **130**, 7244 (2008).

20. I. Boustani, Chem. Phys. Lett. **233**, 273 (1995).

21. I. Boustani, Z. Zhu, and D. l. Tománek, Physical Review B **83**, 193405 (2011).

22. B. C. Hikmat, T. Baruah, and R. R. Zope, J. Phys. B: At. Mol. Opt. Phys. **45**, 225101 (2012).

23. A. D. Becke, The Journal of Chemical Physics **98**, 5648 (1993).

24. A. D. Becke, The Journal of Chemical Physics **98**, 1372 (1993).

25. A. D. Becke, Phys. Rev. A **38**, 3098 (1988).

26. M. J. Frisch, G. W. Trucks, H. B. Schlegel, G. E. Scuseria, M. A. Robb, J. R. Cheeseman, G. Scalmani, V. Barone, B. Mennucci, G. A. Petersson, et al., *Gaussian09 Revision A.02* (Gaussian Inc. Wallingford CT 2016, 2009).

27. D. Y. Zubarev and A. I. Boldyrev, Phys. Chem. Chem. Phys. **10**, 5207 (2008).

28. D. Y. Zubarev and A. I. Boldyrev, The Journal of Organic Chemistry **73**, 9251 (2008).

29. D. Y. Zubarev and A. I. Boldyrev, Journal of Computational Chemistry **28**, 251 (2007).

30. T. Lu and F. Chen, Journal of Computational Chemistry **33**, 580 (2012).

31. M. D. Hanwell, D. E. Curtis, D. C. Lonie, T. Vandermeersch, E. Zurek, and G. R. Hutchison, Journal of Cheminformatics **4**, 17 (2012).

32. G. Schaftenaar and J. Noordik, Journal of Computer-Aided Molecular Design **14**, 123 (2000).

33. A. G. Arvanitidis, T. B. Tai, M. T. Nguyen, and A. Ceulemans, Phys. Chem. Chem. Phys. **16**, 18311 (2014).

34. T. B. Tai, R. W. A. Havenith, J. L. Teunissen, A. R. Dok, S. D. Hallaert, M. T. Nguyen, and A. Ceulemans, Inorganic Chemistry **52**, 10595 (2013).

35. A. N. Alexandrova, A. I. Boldyrev, H.-J. Zhai, and L.-S. Wang, The Journal of Physical Chemistry A **108**, 3509 (2004).

36. A. P. Sergeeva, I. A. Popov, Z. A. Piazza, W.-L. Li, C. Romanescu, L.-S. Wang, and A. I. Boldyrev, Accounts of Chemical Research **47**, 1349 (2014).

37. A. J. Ceulemans, *Group Theory Applied to Chemistry* (Springer, Dordrecht, 2013).

38. A. Kumar, M. Duran, and M. Solá, Journal of Computational Chemistry **38**, 1606 (2017).